Processing and Application of Ceramics 15 [3] (2021) 219–225
https://doi.org/10.2298/PAC2103219Z

Facile preparation of ZrO_2 whiskers by LiF-KCl molten salts synthesis

Quan Zhang[1,2], Guo Feng[2], Feng Jiang[1], Jianmin Liu[2], Lifeng Miao[2], Qian Wu[2], Tao Wang[1], Weihui Jiang[1,2,*]

[1]*School of Material Science and Engineering, Jingdezhen Ceramic Institute, Jingdezhen 333403, China*
[2]*National Engineering Research Center for Domestic & Building Ceramics, Jingdezhen 333001, China*

Received 27 January 2021; Received in revised form 18 April 2021; Accepted 3 July 2021

Abstract

Monoclinic zirconia (ZrO_2) whiskers were made via the molten salt method using zirconyl chloride octahydrate ($ZrOCl_2 \cdot 8\,H_2O$) as zirconium source, potassium chloride (KCl) as molten salt and lithium fluoride (LiF) as a mineraliser. DSC-TG, XRD, FE-SEM, Raman and TEM were performed to study the effects of heat treatment temperature, holding time and heating rate on the synthesis of zirconia whiskers. The results indicate that zirconia whiskers with diameters of 50–80 nm and aspect ratios of 10–30 can be obtained by heating the precursor at slow rate (3 °C/min) to 718 °C for 1 h and then at faster rate (7 °C/min) to 950 °C for 3 h. The whiskers have a smooth surface and grow in [001] direction. The key to the ZrO_2 whiskers growth is the controlled dissolution and precipitation of the ZrO_2 in a LiF-KCl molten salt solution environment.

Keywords: *zirconia whisker, molten salt process, LiF-KCl, growth mechanism*

I. Introduction

ZrO_2 can be applied in catalyst carrier [1], filter membrane [2] and thermal barrier coating [3] due to its high melting point and toughness, good corrosion, wear and oxidation resistance, and a series of other outstanding properties [4–7]. Whisker is a single-crystal material, which can be used in the field of structural materials to reinforce and toughen the matrix phase [8–11]. Zirconia whiskers can be used to strengthen ceramics [12,13]. Simultaneously, since the thermal expansion coefficient of zirconia is close to some metal materials [14], zirconia whiskers are expected to be used as metal alloy reinforcement [15], showing wide application prospects.

Zirconia whiskers were reported to be prepared by chemical vapor deposition (CVD) [15], hydrothermal [16] and molten salt [17–19], so far. The molten salt method is widely used for whisker preparation due to its economy, simple process, low equipment requirements and easy to yield [20]. Earlier, we reported that zirconia whiskers with a high aspect ratio were prepared by using phosphate [17,18] as molten salt. However, phosphate reacts with zirconium to form sodium zirconium phosphate, an impurity that is difficult to remove from the final product. KCl and NaCl are commonly used in the molten salt method due to their environmental protection, stability and low-cost [21–25]. However, the preparation of zirconia whiskers with LiF-KCl as molten salt has not been reported. How to select stable and low-cost LiF-KCl as molten salt through a simple synthesis route to obtain zirconia whiskers is explored and explained in this paper.

II. Experimental

All the chemicals used in this experiment were of analytical grade. A typical experiment started with mixing of 1 g $ZrOCl_2 \cdot 8\,H_2O$, 1 g KCl and 0.08 g LiF in an agate mortar and grinding for 20 min until powders were evenly mixed. The mixture was placed in a corundum crucible with a diameter of 2 cm and height of 6 cm, then placed in a muffle furnace and heated under different conditions to investigate the influence of temperature, holding time and heating rate on characteristics of the final product. Thus, the first set of samples was heated at different temperatures from 200 to 1000 °C for 1 h, whereas the second set of samples was heated at 950 °C with the heating rate of 1–9 °C/min and holding time of 1–9 h. The two-step heating (first at 718 °C with 3 °C/min rate and 1 h dwell then to 950 °C with 7 °C/min for 3 h) was also applied. All prepared samples were cooled to room temperature inside the fur-

* Corresponding author: tel: +86 798 8499328,
e-mail: *whj@jci.edu.cn*

nace, then cleaned repeatedly with deionized water, centrifuged for precipitation for several times until the filtrate conductivity reached 100 S/m and dried at 70 °C.

The compositions were examined by XRD (D8, Bruker) using Cu Kα radiation. Raman spectra were observed using a Renishaw Raman spectrometer in the wavenumber range between 0 and 800 cm^{-1} using the 532 nm line of an argon-ion laser. Simultaneous differential scanning calorimetry (DSC) and thermogravimetry (TG) were performed on a thermogravimetric analyser (STA449C NETZSCH) with the heating rate of 10 °C/min in an air atmosphere. The structure and morphology of the whiskers were investigated using FE-SEM (SU8010, Hitachi High-Technologies Corp.) and TEM (JSM-2010, JEOL), respectively.

III. Results and discussion

Figure 1 shows the thermal analysis curves of the precursor mixture and XRD patterns of the samples heat treated at different temperatures are shown in Fig. 2. There is a weight loss of about 17 wt.% in temperature range from RT to 280 °C in the TG curve and two

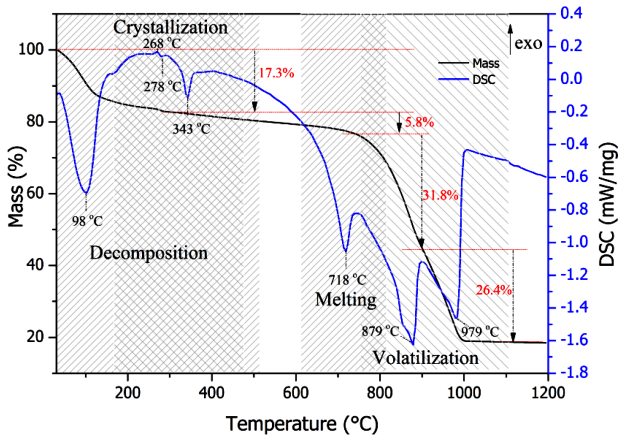

Figure 1. DSC-TG curves of the precursor

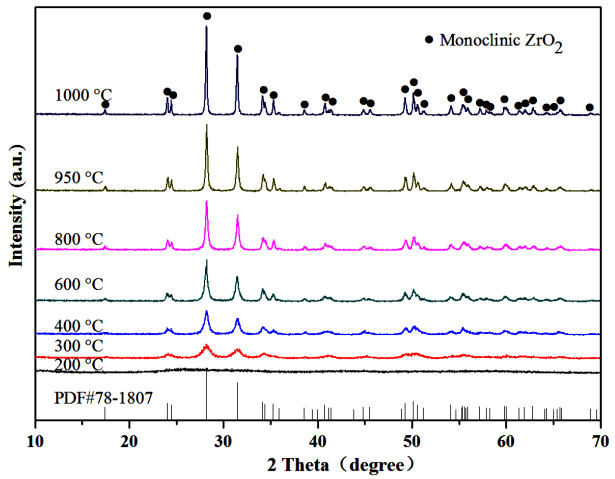

Figure 2. XRD patterns of ZrO_2 heat-treated at different temperatures for 1 h

endothermic peaks at 98 °C and 278 °C in the DSC curve. There is no diffraction peak in the XRD pattern of the sample heated at 200 °C indicating that these two endothermic peaks are related to the removal of crystalline water from $ZrOCl_2 \cdot 8\,H_2O$ [18]. The diffraction peaks of monoclinic zirconia appeared at 300 °C and it is inferred that the exothermic peak of DSC at 268 °C is caused by the transition of zirconia from amorphous to the crystalline state. There are no traces of tetragonal ZrO_2 in the synthesized particles at 300 °C though they are relatively small as documented in Fig. 3a, which may be attributed to the adsorption of fluoride ions [26]. The adsorption of fluoride ions reduces the surface energy of zirconia. Thus, there is no preference for the formation of tetragonal phase and the monoclinic phase appears [27]. The DSC results show an endothermic peak at 718 °C, the TG curve near 718 °C temperature has no obvious weight loss. When compared to the phase diagram of KCl-LiF [28] it can be concluded that the endothermic at 718 °C is caused by the melting of KCl-LiF. The results obtained at 500 °C and 800 °C show no new crystal diffraction peak except monoclinic zirconia, confirming the judgment of endothermic peak at 718 °C. From 800 to 1000 °C, there is a large weight loss, about 58 wt.%, in the TG curve. Combined with the fact that there is no crystal change according to the XRD results of the samples obtained at 800, 950 and 1000 °C, it can be concluded that the volatilization of KCl-LiF is responsible for the endothermic peaks in the DSC curves at 879 °C and 979 °C.

Based on the above thermal analysis and corresponding XRD results at key temperatures, the precursor transformation processes during the heat treatment can be summarized as follows:

$$ZrOCl_2 \cdot 8\,H_2O \xrightarrow[98-600\,^\circ C]{Decomposition} a\text{–}ZrO_2 + 2\,HCl + 7\,H_2O$$

$$a\text{–}ZrO_2 \xrightarrow[268\,^\circ C]{Crystallization} m\text{–}ZrO_2$$

$$KCl_{solid} + LiF_{solid} \xrightarrow[718\,^\circ C]{Melting} KCl\text{–}LiF_{melt}$$

$$m\text{–}ZrO_2 + KCl\text{–}LiF_{melt} \xrightarrow[879\,^\circ C]{Dissolution} ZrO_2\text{–}KCl\text{–}LiF_{melt}$$

$$KCl\text{–}LiF_{melt} \xrightarrow[879-1000\,^\circ C]{Volatilization} KCl\text{–}LiF_{gas}$$

SEM images of the samples acquired at 300–1000 °C are shown in Fig. 3. As shown in Figs. 3a-c, the specimens prepared at temperatures below 718 °C (the melting point of molten salt) are granular. Change from granular to one-dimensional morphology could be observed for the sample prepared at 800 °C (Fig. 3d). When the heat treatment temperature was increased to 950 °C or 1000 °C, the particles show uniform one-dimensional morphology, indicating that the temperature plays a key role in shaping the morphology.

The XRD patterns and SEM images of ZrO_2 heat-treated for different holding times are shown in Figs. 4 and 5, respectively. Figure 4 shows that the holding time

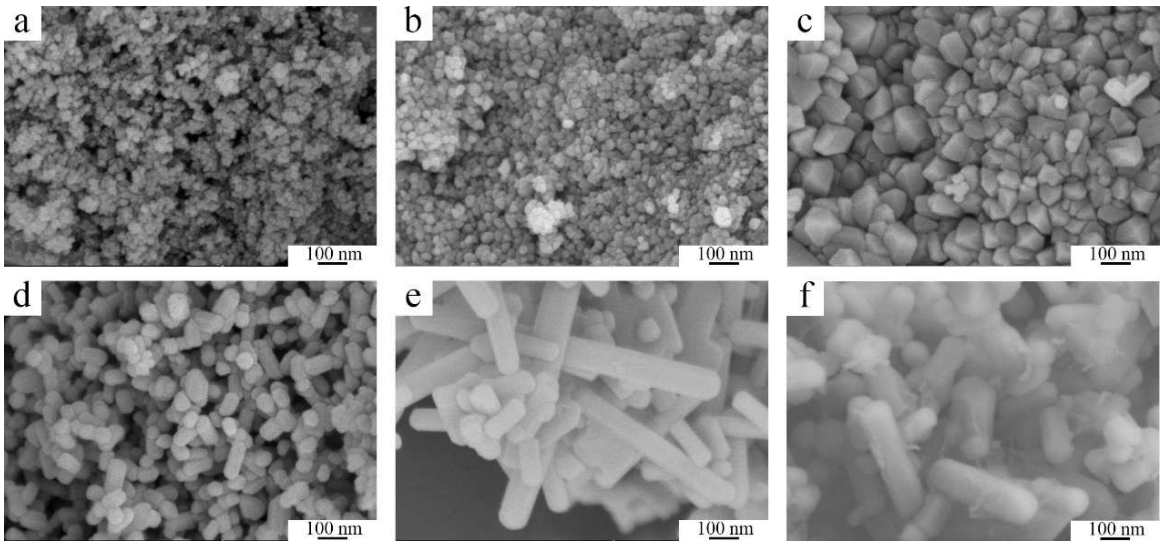

Figure 3. SEM images of ZrO_2 heat-treated 1 h at different temperatures: a) 300, b) 400, c) 600, d) 800, e) 950 and f) 1000 °C

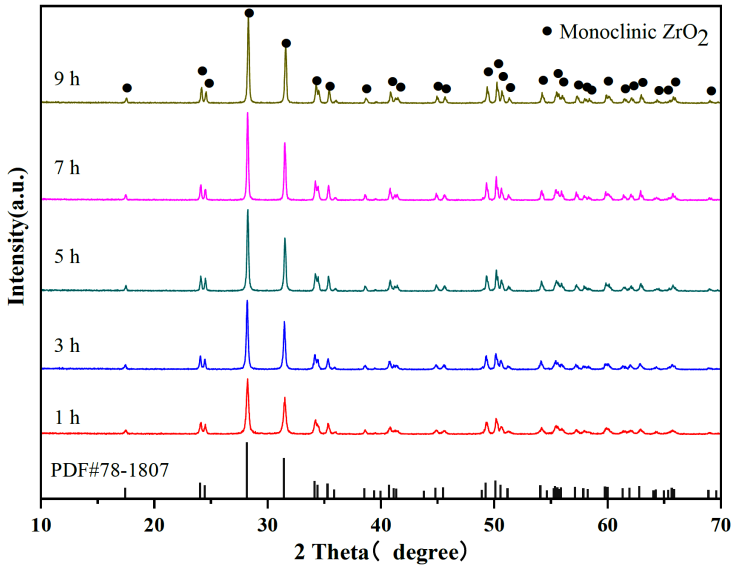

Figure 4. XRD patterns of ZrO_2 heat-treated at 950 °C for different holding time

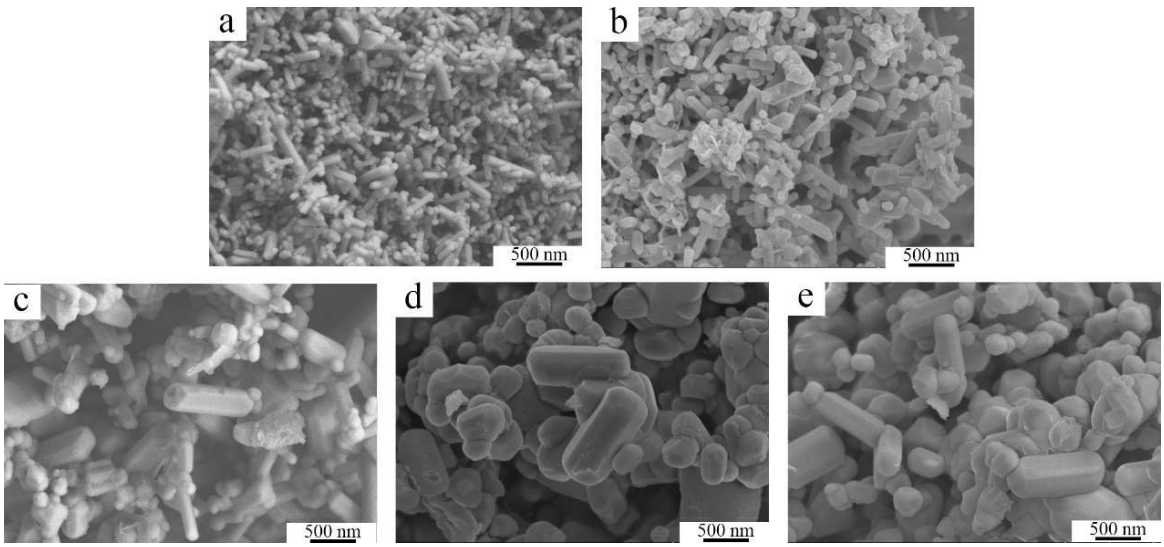

Figure 5. SEM images of ZrO_2 heat-treated at 950 °C for different holding time: a) 1, b) 3, c) 5, d) 7 and e) 9 h

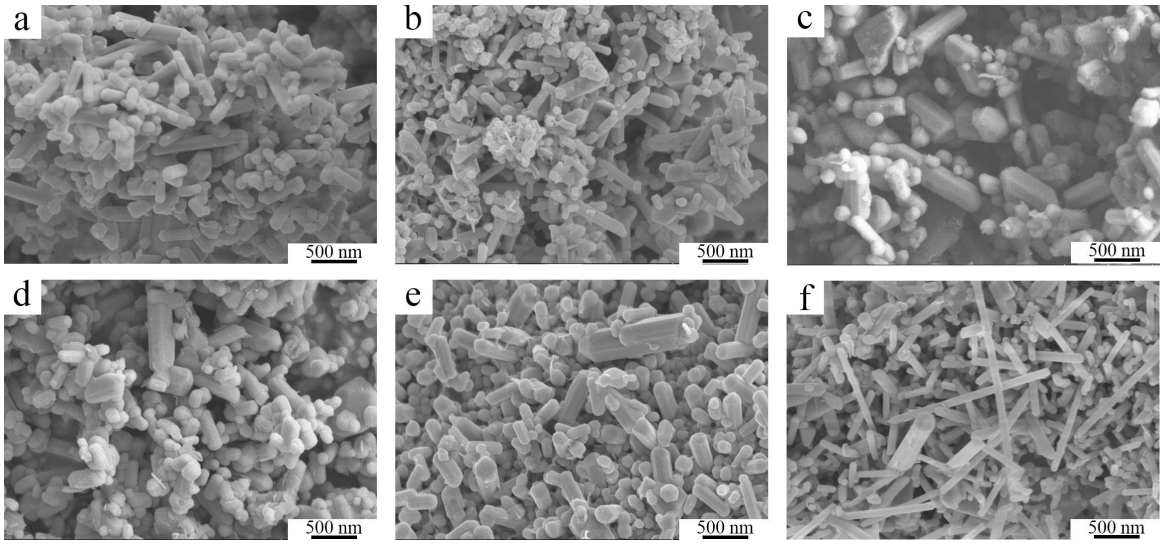

Figure 6. SEM of the samples heated for 3 h at 950 °C with different heating rates: a) 1, b) 3, c) 5, d) 7 and e) 9 °C/min, and f) sample obtained by two-step heating (first at 718 °C for 1 h with 3 °C/min then 7 °C/min to 950 °C)

has little influence on the crystal phase, which are all monoclinic zirconia without diffraction peaks of other crystal phases. Nevertheless, the influence of the holding time on the morphology of the final samples is considerable. The morphology of the sample obtained by holding time of 1 h is rod-shaped. There are a couple of whiskers obtained by soaking time of 3 h. When the heat preservation time is prolonged, the particle morphology is characterized by short rods. The reason for this phenomenon may be that when the heat holding time is short, the crystal growth time is short, and the samples are fine with short rods. With the extension of the holding time, the rods grow into whiskers. When the holding time is too long, the whiskers grow along the radial direction, and the crystals appear as short rods.

Figure 6 presents SEM images of the ZrO_2 prepared with different heating rates. When the heating rate is slow, the particles are small and uniform rod-like particles (Figs. 6a,b). When the heating rate is too fast the obtained samples have different morphologies, such as rod-shaped, small particles and large particles (Figs. 6c,d,e).

The reaction might be as follows. The precursor decomposes at a low temperature (below 600 °C) and the

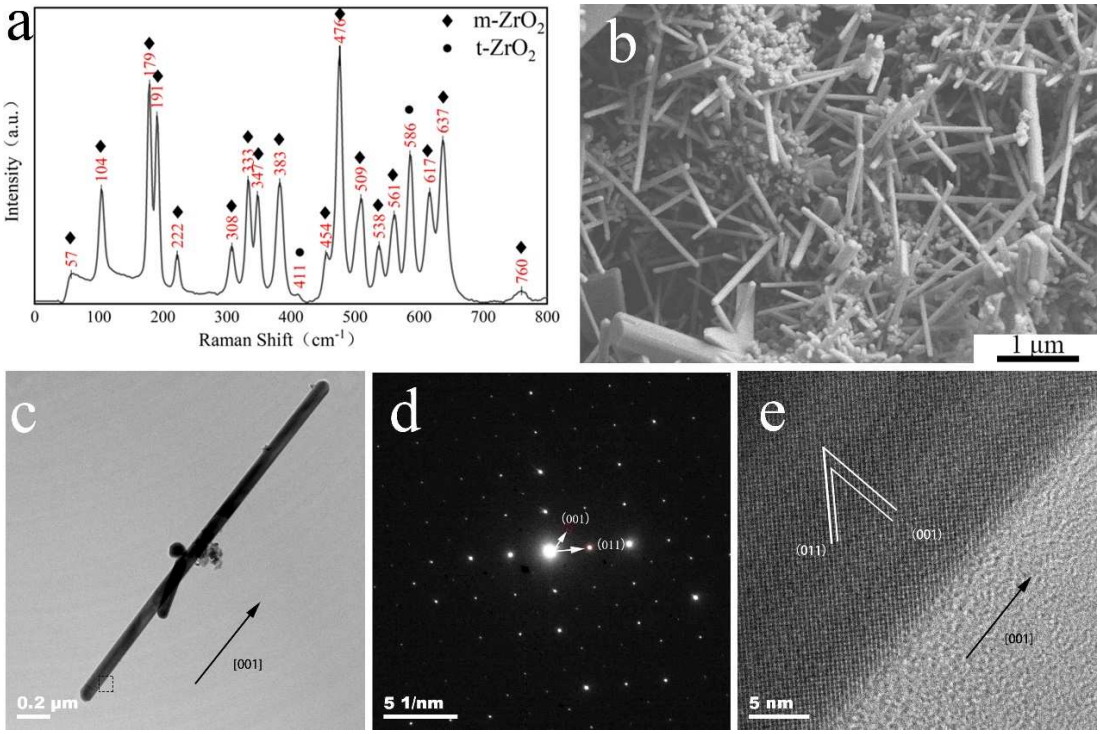

Figure 7. Characterization of as-synthesized ZrO_2 whiskers prepared by two-step heating: a) Raman spectrum, b) FE-SEM, c) TEM image, d) SAED pattern and e) HR-TEM image

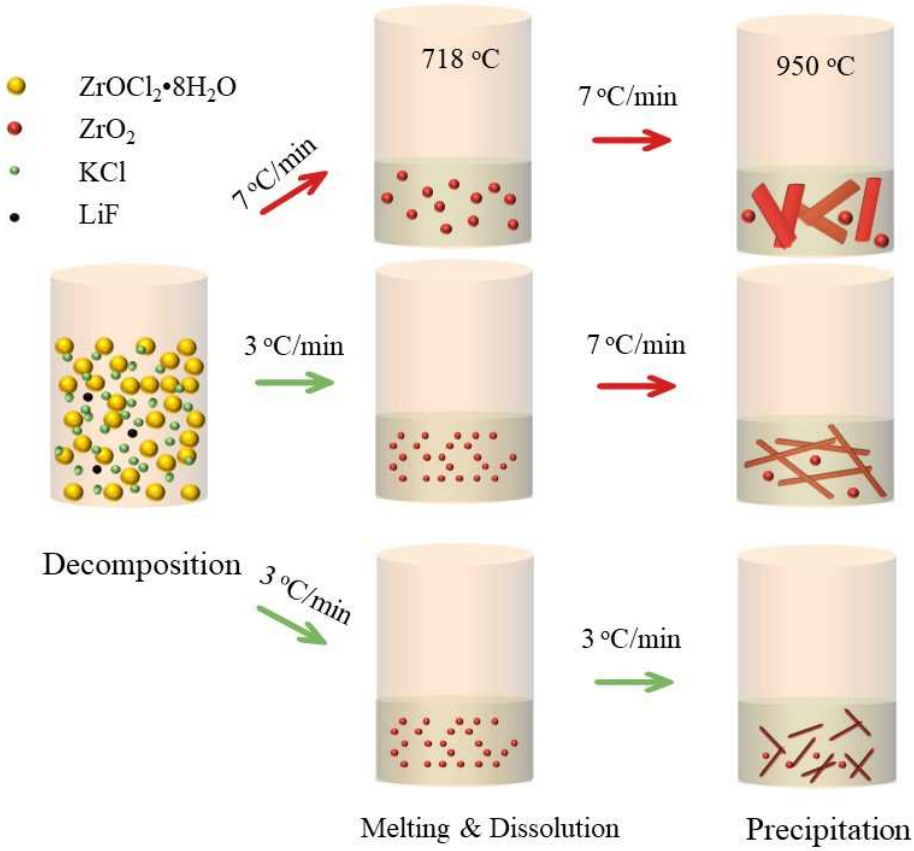

Figure 8. Illustration of the protocol for a simple model for the synthesis of ZrO_2 whiskers

molten salt melts near the melting point (718 °C). The decomposition product of the precursor dissolves in the molten salt and then precipitates in the saturated liquid phase. When the heating rate is too slow, the precursor completely decomposes before the molten salt melts. At the same time, the heating rate is slow and the time required to reach the same temperature is long. As the crystal particles grow, it is difficult for the large particles to dissolve in molten salt and finally they stay in the product. When the heating rate is too fast, the decomposition products of precursor dissolve in molten salt and then many uniform nuclei precipitate and grow into rods.

If different heating rates are used before and after molten salt melting, zirconia whiskers with a certain aspect ratio may be obtained, as shown in Fig. 6f. Below the melting point of the molten salt (718 °C), a slower heating rate of 3 °C/min was selected to make the precursor fully decompose. After molten salt melting, the heating rate was increased (7 °C/min) to avoid crystal growth and ensure a more uniform zirconia whiskers.

Figure 7 presents Raman spectrum of the whisker sample prepared by two-step heating (Fig. 7a), and their corresponding SEM image, TEM image, SAED pattern and HR-TEM image are shown in Figs. 7b,c,d,e, respectively. The SEM photograph shows that the sample is mainly composed of whiskers. The Raman pattern shows that the main phase was monoclinic zirconia, without obvious hetero-peaks. Combined with the XRD standard card (PDF# 78-1807) *d* value, it indicates that the growth direction of the zirconia whisker is [001]. SEM and TEM images (Figs. 7b,c) also show that whiskers are below 100 nm in diameter with the aspect ratios between 10–30.

A schematic diagram of the growth process of zirconia whisker is illustrated in Fig. 8. That is, the precursor raw materials are first mixed evenly in mortar. The precursor $ZrOCl_2 \cdot 8\,H_2O$ decomposes into small ZrO_2 particles during the heating. Potassium chloride and lithium fluoride melt and form a liquid phase at about 718 °C. The heating stops and the sample forms zirconia whisker as the furnace cools. When the heating rate is relatively slow (e.g. 3 °C/min), the time to reach the same temperature is longer. The decomposition of precursors is sufficiently high. After molten salt melting, zirconia is dissolved in the molten salt completely. Zirconia is supersaturated to precipitate into fine and uniform rod-like particles. When the heating rate is relatively fast (e.g. 7 °C/min), it takes a short time to reach the same temperature. Only part of the zirconia is dissolved in the molten salt, and the dissolved zirconia precipitates into rod-like particles, while the undissolved zirconia grows into large particles. When the two-step heating rate is selected, the first heating rate is slow and contributes to the complete decomposition of the precursor. Then, the molten salt is already melted and the heating rate is increased which enables shortening of the time needed to reach the maximum temperature. The

heating stage completes more quickly and the cooling stage starts earlier. This causes zirconia to supersaturate in the molten salt providing a certain driving force for the growth of crystals. Finally, the whisker-like particles are obtained.

IV. Conclusions

In this paper, a simple LiF-KCl molten salts synthesis method was used for preparation of ZrO_2 whiskers. The effects of heat treatment temperature, holding time and heating rate on the synthesis of zirconia whiskers were studied. The results show that the zirconia whiskers with a diameter of 50–80 nm and aspect ratios of 10–30 could be obtained through the careful precursor processing: heating at a slow rate (3 °C/min) at first and then accelerating (7 °C/min) above salt melting temperature (718 °C), and final holding for 3 h at 950 °C. The surface is smooth without obvious defects with whiskers growing in the [001] direction. The patterns of XRD and Raman spectrum show monoclinic ZrO_2 without impurities. The formation mechanism of zirconia whisker could be described with the precursor and molten salt undergoing decomposition and melting processes, respectively, as the heating temperature rises. Then the decomposed precursor products dissolve in molten salt, zirconia grows preferentially in [001] direction because of the anisotropic nature of its monoclinic structure and thus whiskers are formed.

Acknowledgements: This work was supported by the National Natural Science Foundation of China (grant numbers 52072162, 51962014); Jiangxi Provincial Natural Science Foundation (grant numbers 20202ACBL214006, 20202ACBL214008, 20192BBEL50022, 2020ZDI03004, 20202BABL214013); Open fund project of the Key Laboratory of Inorganic Coating Materials, Chinese Academy of Science (ICM-202001); the Jingdezhen science and technology plan project (20202GYZD013-09, 20202GYZD013-14); the Science Foundation of Jiangxi Provincial Department of Education (GJJ201324, GJJ201345).

References

1. K. Larmier, W.C. Liao, S. Tada, E. Lam, R. Verel, A. Bansode, A. Urakawa, A. Comas-Vives, C. Copéret, "CO_2-to-methanol hydrogenation on zirconia-supported copper nanoparticles: Reaction intermediates and the role of the metal-support interface", *Angew. Chem. Int. Ed.*, **56** [9] (2017) 2318–2323.
2. N. Maximous, G. Nakhla, W. Wan, K. Wong, "Performance of a novel ZrO_2/PES membrane for wastewater filtration", *J. Membr. Sci.*, **352** [1-2] (2010) 222–230.
3. R. Vassen, X. Cao, F. Tietz, D. Basu, D. Stöver, "Zirconates as new materials for thermal barrier coatings", *J. Am. Ceram. Soc.*, **83** [8] (2000) 2023–2028.
4. G. Feng, W. Jiang, J. Liu, Q. Zhang, L. Miao, "A novel green nonaqueous sol-gel process for preparation of partially stabilized zirconia nanopowder", *Process. Appl. Ceram.*, **11** [3] (2017) 220–224.
5. M. Zhou, L. Xu, X. Xi, P. Li, W. Dai, W. Zhu, A. Shui, L. Zeng, "Investigation on the preparation and properties of monodispersed Al_2O_3-ZrO_2 nanopowder via Co-precipitation method", *J. Alloys Compd.*, **678** (2016) 337–342.
6. E. Ferraris, T. Mestrom, R. Bian, D. Reynaerts, B. Lauwers, "Machinability investigation on high speed hard turning of ZrO_2 with PCD tools", *Procedia Cirp*, **1** [1] (2012) 500–505.
7. M. Biswas, S. Bandyopadhyay, "Zirconia fiber via biotemplate synthesis route", *Mater. Lett.*, **101** (2013) 13–16.
8. I. Balázs, S. Agata, R. Jacek, D. Karel, B. David, "The influence of the crystallographic structure of the intermetallic grains on tin whisker growth", *J. Alloys Compd.*, **785** (2019) 774–780.
9. Y. Fang, N. Chen, G. Du, M. Zhang, X. Zhao, J. Wu, "Effect of Y_2O_3-stabilized ZrO_2 whiskers on the microstructure, mechanical and wear resistance properties of Al_2O_3 based ceramic composites", *Ceram. Int.*, **45** [13] (2019) 16504–16511.
10. F. Zuo, F. Meng, D.-T. Lin, J.-J. Yu, H.-J. Wang, S. Xu, W.-M. Guo, C. Cerecedo, V. Valcárcel, H.-T. Lin, "Influence of whisker-aspect-ratio on densification, microstructure and mechanical properties of Al_2O_3 whiskers-reinforced CeO_2-stabilized ZrO_2 composites", *J. Eur. Ceram. Soc.*, **1** [4] (2018) 1796–1801.
11. G. Feng, F. Jiang, W. Jiang, J. Liu, S. Wang, Q. Zhang, L. Miao, Q. Wu, "Preliminary study on the growth mechanism of zircon whiskers prepared via non-hydrolytic sol-gel method combined with carbon black as reducing agent", *Process. Appl. Ceram.*, **12** [2] (2018) 95–99.
12. S. Li, C. Wei, P. Wang, P. Gao, L. Zhou, G. Wen, "Fabrication of ZrO_2 whisker modified ZrO_2 ceramics by oscillatory pressure sintering", *Ceram. Int.*, **46** [11] (2020) 17684–17690.
13. Y. Fang, X. Zhao, M. Zhang, P. Zhang, H. Cheng, S. Xue, L. Zhang, J. Wu, S. Feng, "Effect of ZrO_2 whiskers on the microstructure and mechanical properties of a Ti(C,N)-based cermet cutting tool material", *Int. J. Appl. Ceram. Technol.*, **16** [4] (2019) 1347–1355.
14. R.H. Hannink, P.M. Kelly, B.C. Muddle, "Transformation toughening in zirconia-containing ceramics", *J. Am. Ceram. Soc.*, **83** [3] (2000) 461–487.
15. D.B. Epassaka, S. Ohshio, H. Saitoh, "Morphological instability of ZrO_2 crystallites formed by CVD technique operated under atmospheric pressure", *J. Mater. Sci.*, **38** [15] (2003) 3239–3244.
16. E. Kato, A. Nagai, M. Hirano, Y. Kobayashi, "Growth of whiskered ZrO_2 crystals by hydrothermal decomposition of zirconium oxide sulphate pseudo-crystals", *J. Mater. Sci.*, **32** [7] (1997) 1789–1794.
17. T. Wang, J. Liu, W. Jiang, G. Feng, L. Miao, T. Chen, Q. Wu, H. Tang, W. Luo, "Facile molten salt synthesis of zirconia whiskers", *Process. Appl. Ceram.*, **12** [3] (2018) 257–261.
18. W. Tao, J. Weihui, L. Jianmin, F. Guo, M. Lifeng, C. Ting, W. Qian, "Simple and novel synthesis of zirconia whiskers from a phosphate flux", *Ceram. Int.*, **45** [4] (2019) 4514–4519.
19. Y.-H. Fang, X.-R. Zhao, M.-X. Zhang, P. Zhang, L. Zhang, H. Cheng, J.-B. Wu, S.-S. Feng, "Preparation and char-

acterization of monoclinic rod-shaped ZrO_2 whiskers via sulfate flux", *Ceram. Int.*, **44** [9] (2018) 10094–10098.
20. M.A. Einarsrud, T. Grande, "1D oxide nanostructures from chemical solutions", *Chem. Soc. Rev.*, **43** [7] (2014) 2187–2199.
21. T. Katsuya, N. Yuki, Y. Kunio, S. Takaomi, I. Nobuo, S. Toetsu, O. Shuji, "Environmentally friendly growth of layered $K_4Nb_6O_{17}$ crystals from a KCl flux", *Eur. J. Inorg. Chem.*, **2007** [29] (2007) 4687–4692.
22. K. Teshima, K. Yubuta, T. Shimodaira, T. Suzuki, M. Endo, T. Shishido, S. Oishi, "Environmentally friendly growth of highly crystalline photocatalytic $Na_2Ti_6O_{13}$ whiskers from a NaCl flux", *Cryst. Growth Des.*, **8** [2] (2008) 465–469.
23. X. Liu, G. Feng, J. Liu, F. Jiang, T. Chen, J. Liang, L. Miao, W. Jiang, "Effect of NaOH on the preparation of two-dimensional flake-like zirconia nanostructures", *Chem. Phys. Lett.*, **754** (2020) 137755–137762.
24. X. Liu, T. Wang, J. Liu, F. Jiang, H. Tang, G. Feng, W. Jiang, "Preparation, characterization and growth mechanism of ZrO_2 nanosheets", *Ceram. Int.*, **46** [4] (2020) 4864–4869.
25. J. Liu, T. Wang, W. Jiang, G. Feng, L. Miao, T. Chen, Q. Wu, S. Wang, "Preparation, characterization and formation mechanism of single-crystal zirconia micro-sheets", *Process. Appl. Ceram.*, **13** [3] (2019) 229–234.
26. P. Afanasiev, "Synthesis of dispersed ZrO_2 in the fluoride-doped molten $NaNO_3$-KNO_3 mixtures", *J. Mater. Sci. Lett.*, **16** [20] (1997) 1691–1692.
27. M. Bremholm, J. Becker-Christensen, B.B. Iversen, "High-pressure, high-temperature formation of phase-pure monoclinic zirconia nanocrystals studied by time-resolved in situ synchrotron X-ray diffraction", *Adv. Mater.*, **21** [35] (2009) 3572–3575.
28. S. Maji, S. Kumar, K. Sundararajan, K. Sankaran, "Feasibility study for quantification of lanthanides in LiF-KCl salt by laser induced breakdown spectroscopy", *J. Radioanal. Nucl. Chem.*, **314** [2] (2017) 1279–1285.